Bioscience, Biotechnology, and Biochemistry, 2026, **90**, 1317–1326
https://doi.org/10.1093/bbb/zbag106
Advance access publication date: 16 July 2026
Regular Paper

Synthesis, cytotoxicity, and pyoverdine production inhibitory activity of actinomycin lactam analogs

Kenta Yamanoue[1], Yasumasa Hara[2], Ryo C. Yanagita[2], and Yusuke Hanaki[2,*]

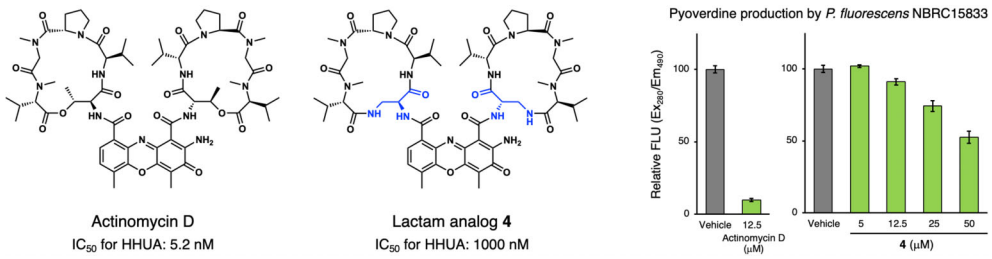
[1]Department of Applied Bioresource Science, The United Graduate School of Agricultural Sciences, Ehime University (Kagawa University), Kagawa, Japan
[2]Department of Applied Biological Science, Faculty of Agriculture, Kagawa University, Kagawa, Japan
*Correspondence: Yusuke Hanaki, hanaki.yusuke@kagawa-u.ac.jp

Abstract

Pyoverdines are fluorescent siderophores and potential virulence factors produced by *Pseudomonas* bacteria. Actinomycin D has been reported to inhibit pyoverdine production; however, its strong cytotoxicity limits its use as a probe to elucidate pyoverdine function. In this study, we synthesized actinomycin analogs (**1**–**4**) with a modified phenoxazine moiety. To enable convergent syntheses, the threonine residues were replaced with 2,3-diaminopropionic acid. Compounds **1**–**4** showed negligible to low cytotoxicity toward HHUA endometrial cancer cells. However, only **4**, with the same phenoxazine ring as actinomycin D, retained inhibitory activity against pyoverdine production by *Pseudomonas fluorescence* NBRC15833, although an order of magnitude lower than actinomycin D. These results suggest that the phenoxazine ring would be essential to the cytotoxicity and pyoverdine production inhibitory activity, and the further modification of the cyclic peptide moiety is necessary to understand the structure–activity relationship underlying pyoverdine production inhibition.

Keywords: actinomycin, pyoverdine, Pseudomonas, cytotoxicity, structure–activity relationship

Graphical abstract



Four actinomycin lactam analogs were synthesized. The less toxic analog **4** suppressed pyoverdine production.

Iron is essential for the survival and growth of most organisms because of its pivotal role in processes such as nucleic acid synthesis and energy production. Thus, bacteria and plants produce siderophores, i.e. specialized molecules that chelate and facilitate iron uptake (Crowley *et al.* 1991). Pyoverdines are fluorescent siderophores synthesized by select *Pseudomonas* species, with more than 100 derivatives identified so far (Visca, Imperi and Lamont 2007). They consist of a 2,3-diamino-6,7-dihydroquinoline fluorescent chromophore, a variable peptide chain containing 6–12 amino acids, and an acyl side chain bound to the amino group at position 3 of the chromophore.

Pyoverdine production is crucial for the survival of many *Pseudomonas* species. For example, *Pseudomonas syringae* pv. tabaci 6605, a plant pathogen that causes wildfire disease in tobacco plants, exhibits significantly reduced virulence on host plants when pyoverdine biosynthesis is disrupted, accompanied by reduced virulence factor and quorum-sensing molecule productions (Taguchi *et al.* 2010). Similarly, a pyoverdine-deficient mutant of *Pseudomonas fluorescens* PF08 displays impaired biofilm formation, increased motility, and reduced spoilage capacity (Chen *et al.* 2023). Meanwhile, in the opportunistic pathogen *Pseudomonas aeruginosa*, the pyoverdine-deficient mutant exhibits a lower growth rate in transferrin-containing media (Minandri *et al.* 2016). Moreover, pyoverdines secreted by *P. aeruginosa* promote virulence factor production, such as exotoxin A, endoproteases, and pyoverdine itself (Lamont *et al.* 2002). Collectively, these findings suggest that pyoverdines function as iron scavengers and signaling molecules to regulate protein production; this dual functionality suggests that additional roles of pyoverdine remain to be elucidated. Therefore, pyoverdine production inhibitors represent valuable tools for uncovering these functions and may serve as promising candidates for the development of antimicrobial agents and agricultural pesticides.

Recently, several small pyoverdine-inhibiting compounds were discovered by high-throughput screening using a liquid killing assay (Kirienko, Kang and Kirienko 2018). These compounds reduced pyoverdine pathogenic effects and improved the survival of *Caenorhabditis elegans* exposed to *P. aeruginosa* PA14, although

Received: 27 May 2026; **Accepted:** 13 July 2026
© The Author(s) 2026. Published by Oxford University Press on behalf of Japan Society for Bioscience, Biotechnology, and Agrochemistry. This is an Open Access article distributed under the terms of the Creative Commons Attribution License (https://creativecommons.org/licenses/by/4.0/), which permits unrestricted reuse, distribution, and reproduction in any medium, provided the original work is properly cited.

Downloaded from academic.oup.com/bbb/article/90/10/1317/8735818 by guest on 26 September 2026

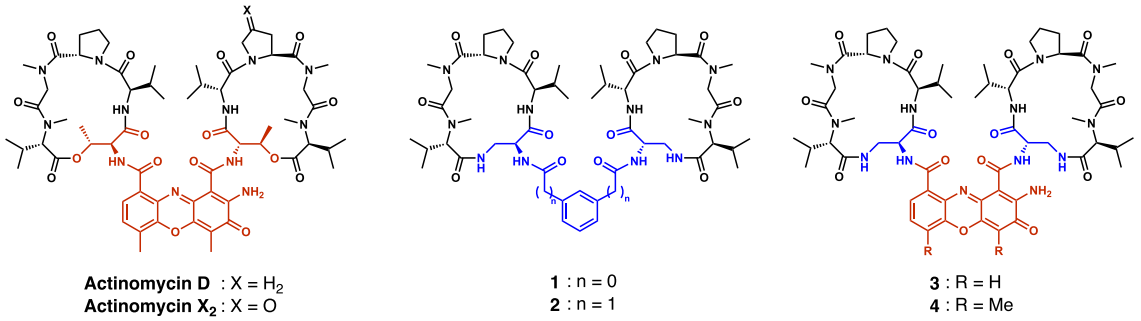


Figure 1. Structure of actinomycins and their analogs (**1**–**4**).

at several hundred micromolar concentrations. These compounds were suggested to directly interact with pyoverdines rather than affect their biosynthesis (Wang *et al.* 2020). Meanwhile, Maenaka et al. screened microbial culture extracts in a pyoverdine-biosynthesis inhibition assay using *Pseudomonas cichorii* SPS9018, a multihost plant pathogen. As a result, actinomycins D and X_2 (Figure 1) were isolated as active components from a *Streptomyces sp.* RM-32 culture extract (Maenaka *et al.* 2020). Additionally, they inhibited pyoverdine production in other *Pseudomonas* bacteria, such as *P. putida*, *P. fluorescens*, *P. chlororaphis*, and *P. tolaasii*, at several tens of micromolar concentrations. Actinomycins were first isolated as antibiotics from actinomycetes (Waksman and Woodruff 1940). Actinomycin D complexes with DNA and inhibits RNA synthesis (Takusagawa *et al.* 1982), thereby showing potent cytotoxicity to mammalian cells and antibacterial activity against Gram-positive bacteria at nanomolar concentrations (Kirk 1960). It was also attempted to evaluate whether the actinomycins suppressed the virulence of *P. cichorii* SPC9018 on eggplant leaves (Maenaka *et al.* 2020). However, the *in vivo* effectiveness could not be determined due to the strong phytotoxicity of the actinomycins to eggplant leaves. As micromolar actinomycin concentrations are required for pyoverdine production inhibitor activity, nanomolar cytotoxicity masks their beneficial pyoverdine inhibition effects. With this in mind, we herein aimed to develop new actinomycin analogs that have reduced cytotoxicity but retain their pyoverdine production inhibitory activity.

Results and discussion

Design and synthetic route for actinomycin analogs

The structure–activity relationship underlying actinomycin-mediated pyoverdine production inhibitory activity remains unknown. However, we hypothesized that the cyclic depsipeptide moiety, rather than the phenoxazine ring, is primarily responsible for the pyoverdine production inhibitory activity. This assumption was based on the similarity in size between actinomycin's cyclic peptide component and pyoverdine's peptide moiety, suggesting a potential interaction with enzymes involved in pyoverdine biosynthesis.

To test this hypothesis, we designed new actinomycin analogs (**1**–**3**) with modifications to the phenoxazine moiety (Figure 1). In native actinomycins, this moiety is essential for DNA intercalation within the actinomycin–DNA complex. Furthermore, methyl substituents on the phenoxazine ring are known to contribute to DNA-binding affinity, as their removal or replacement with other functional groups reduces biological activity (Brockmann and Seela 1971; Yao *et al.* 2021). Therefore, analogs **1**–**3** were expected to be less toxic due to their lack of affinity for DNA.

The threonine residues in both cyclic depsipeptides were replaced with 2,3-diaminopropionic acid to improve synthetic accessibility. Total syntheses of actinomycins have been reported by several groups, typically involving the synthesis of a linear pentapeptide in which the threonine amino group was first condensed with a substituted benzoic acid, followed by cyclization between proline or methylvaline with sarcosine, and subsequent oxidative dimerization yielding actinomycins (Meienhofer 1970; Mauger *et al.* 1985; Mauger, Stuart and Katz 1991).

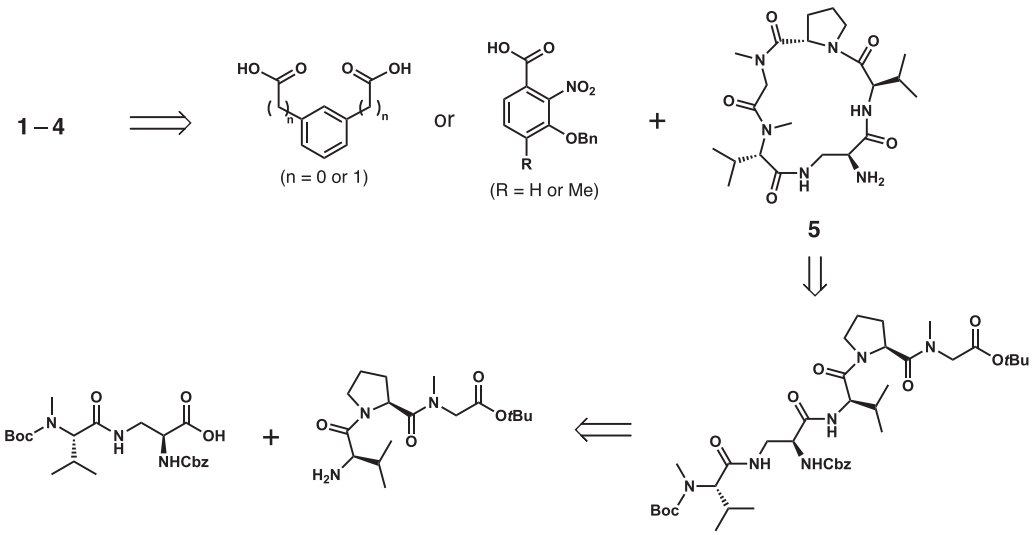
For the collective synthesis of actinomycin analogs (**1**–**3**), a practical strategy is to first prepare the cyclic depsipeptide and then introduce the respective carboxylic acid linkers at a late stage (Scheme 1). A potential limitation of this approach is that cyclic depsipeptides bearing a free amino group are prone to undergo an *O* to *N* acyl shift (Figure 2) (Mauger and Stuart 1987). Although such nonprotected cyclic depsipeptides have been used as intermediates in the actinomycin synthesis (Mosher *et al.* 1979; Nakajima *et al.* 1982; Chu *et al.* 1994), they may need to be stored in a protonated state under acidic conditions or used immediately in the next reaction. Therefore, to avoid these inconveniences, we used the common cyclic peptide **5** (Figure 2).

Additionally, we prepared lactam analog **4** to validate the effects of replacement on the pyoverdine production inhibitory activity; **4** was previously synthesized and found to retain toxicity and antitumor activity at about half the potency of actinomycin D in model mice (Meienhofer and Patel 1971). Moore et al. reported that **4** exhibited significant antibacterial activity, though its potency was significantly, i.e. several to ten times, lower than that of actinomycin D. Additionally, **4** showed a decreased antitumor activity and a slightly higher toxicity to mice compared to actinomycin D (Moore *et al.* 1976). Spectroscopic characterization showed that the circular dichroism of **4** differed from that of actinomycin D, while each compound had a similar spectrum in the presence of DNA. Although there is no clarification on the lactone-to-lactam replacement effect on biological activities, we predicted that the orientation or conformation of cyclic peptides in **4** partly differed from those of the cyclic depsipeptides in actinomycin D; however, they can adopt similar orientations and conformations when bound to a target molecule. Therefore, we assumed that the lactone analogs (**1**–**4**) could inhibit pyoverdine production similar to actinomycin D.

Synthesis of 1–4

The synthesis of **1**–**4** is outlined in Scheme 2. Methylation of N_α-Cbz-L-2,3-diaminopropionic acid, condensation with *N*-Boc-

Downloaded from academic.oup.com/bbb/article/90/10/1317/8735818 by guest on 26 September 2026



Scheme 1. Retrosynthetic analysis of **1**–**4**.

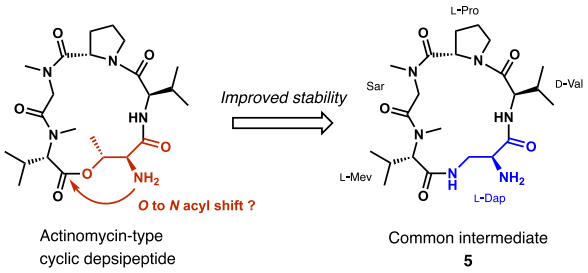


Figure 2. Design of the common intermediate **5**.

L-valine using 1-ethyl-3-(3-dimethylaminopropyl)carbodiimide (EDC) and 1*H*-1,2,3-benzotriazol-1-ol (HOBt), and hydrolysis of the methyl ester yielded dipeptide **9**. Subsequent condensation of **9** with tripeptide **10** (Mauger *et al.* 1985) using EDC and HOBt yielded linear pentapeptide **11**. Deprotection of Boc and tBu groups by HCl, cyclization with 1-[bis(dimethylamino)methylene]-1*H*-1,2,3,-triazolo[4,5-*b*]pyridinium 3-oxide hexafluorophosphate (HATU), and deprotection of the Cbz group yielded a common cyclic pentapeptide **5**. Condensation of **5** with isophthalic acid and 1,3-benzeneacetic acid yielded **1** and **2**, respectively. Condensation of **5** with 2-nitro-3-(phenylmethoxy)benzoic acid and 4-methyl-2-nitro-3-(phenylmethoxy)benzoic acid, followed by hydrogenation and oxidative dimerization using potassium hexacyanidoferrate(III), yielded **3** and **4**, respectively.

Previously, NMR spectra of actinomycin D indicated that each cyclic depsipeptide exists as a single conformer (Bai *et al.* 2019). However, the NMR data for cyclic peptide **5** and analog **4** have not yet been reported, likely due to the low usage of high-resolution NMR analysis when these compounds were synthesized in the 1970s. In this study, the ^{1}H NMR spectrum of **5** indicated that it existed as a mixture of one major and a few minor conformers. In addition, the ^{1}H NMR spectra of **1**–**4** showed broadened peaks, and their ^{13}C NMR spectra gave a larger number of weak peaks than the number of carbon atoms in each compound. Therefore, the lactone to lactam replacement may increase the rotating barrier, resulting in the presence of several conformers of **5**, while **1**–**4** may exist in equilibrium between multiple conformers, as each cyclic peptide can adopt multiple conformations.

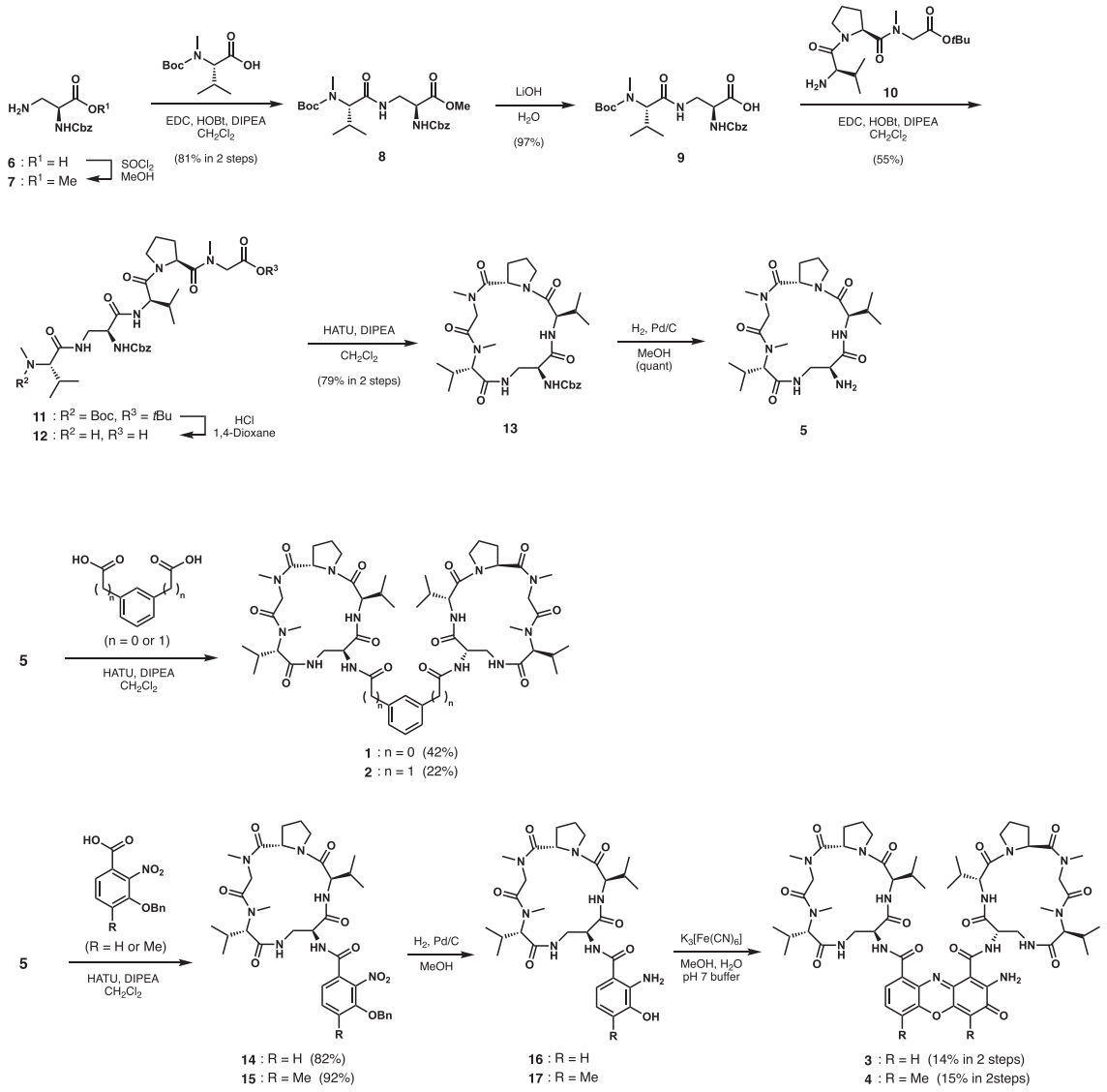
Cytotoxicity of 1–4

We evaluated the cytotoxicity of **1**–**4** in HHUA endometrial cancer cells using a water-soluble tetrazolium salt (WST)-based colorimetric assay (Figure 3). Consistent with previous reports, actinomycin D potently reduced HHUA cell viability (IC_{50} = 5.2 nM). In contrast, **1** and **2** showed no detectable cytotoxicity even at 50 μM. The phenoxazine moiety appears to be essential to their cytotoxicity, as **3** and **4** exhibited significant cytotoxicity (IC_{50} = 4.2 and 1.0 μM, respectively). However, their cytotoxicity was two orders of magnitude lower than that of actinomycin D. The conformational change caused by replacement of threonine with 2,3-diaminopropionic acid might reduce the affinity for DNA because the C=O and N–H groups of the threonine residue form hydrogen bonds with guanine at the DNA intercalation site (Kamitori and Takusagawa 1994). On the other hand, these results were partially inconsistent with previous reports, which indicated that the toxicity and antitumor activities of **4** were only a few times weaker than those of actinomycin D (Meienhofer and Patel 1971; Moore *et al.* 1976). This discrepancy may be due to the difference in cell lines and evaluation methods. Overall, however, we successfully obtained actinomycin analogs with reduced cytotoxicity.

Pyoverdine production inhibitory activity of 1–4

The pyoverdine production inhibitory activity of **1**–**4** was evaluated according to a previously reported method (Maenaka *et al.* 2020). We selected *P. fluorescens* NBRC15833 because actinomycin D strongly inhibits pyoverdine production in this strain. As shown in Figure 4, **1**–**3** showed no significant inhibitory activity even at 50 μM. However, **4** showed a dose-dependent inhibitory effect, though its potency was an order of magnitude weaker than that of actinomycin D; at 50 μM, **4** reduced the relative fluorescence intensity to 53% of the non-treated control. Thus, the lactone to lactam replacement may reduce the affinity for target molecules involved in the pyoverdine production inhibitory activity. Although **4** contained trace impurities despite purification by column chromatography followed by PTLC, we considered that the pyoverdine inhibitory activity was unlikely attributed to these impurities. This is because **3**, which was synthesized and purified using the same procedures and also contained impurities, did not inhibit the pyoverdine production.

Downloaded from academic.oup.com/bbb/article/90/10/1317/8735818 by guest on 26 September 2026



Scheme 2. Synthesis of **1**–**4**.

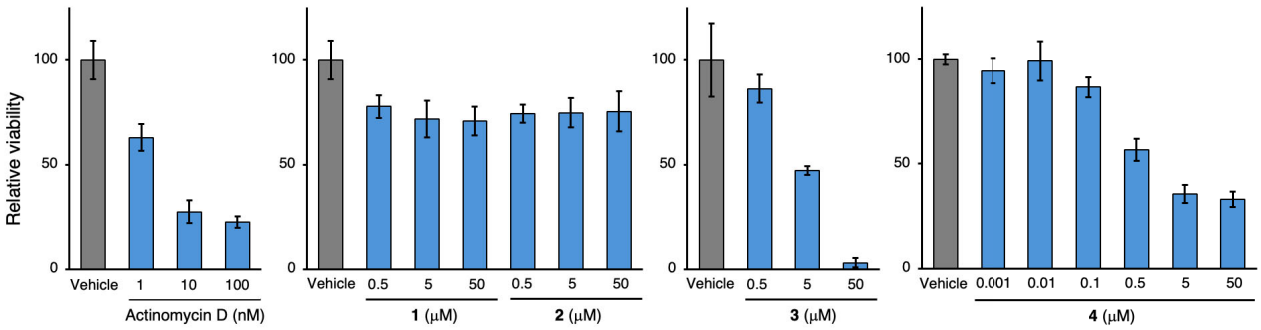


Figure 3. Cytotoxicity of **1**–**4** against HHUA endometrial cells. The cell viability was expressed as a percentage relative to that of the vehicle group. The error bars represent the SD ($n = 3$–5).

Contrary to our hypothesis, these results suggested that the methyl-substituted phenoxazine ring, which intercalates into the DNA duplex, was essential to pyoverdine production inhibition. Therefore, actinomycins might suppress pyoverdine production by inhibiting the transcription of pyoverdine biosynthetic genes. As mentioned above, the cytotoxicity of **4** was approximately 200 times lower than that of actinomycin D. The smaller decrease in pyoverdine production inhibitory activity than the decrease in cy-

Downloaded from academic.oup.com/bbb/article/90/10/1317/8735818 by guest on 26 September 2026

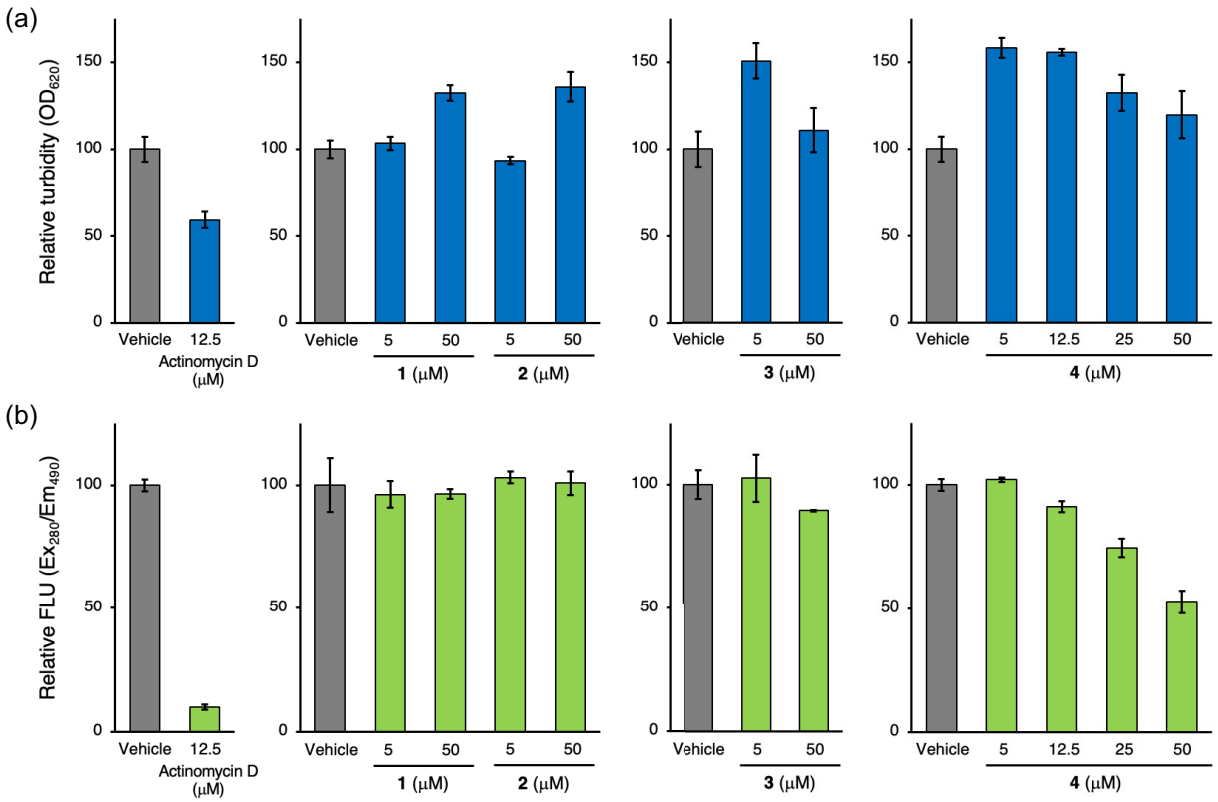


Figure 4. Inhibitory activities of **1**–**4** on growth and pyoverdine production of *P. fluorescens* NBRC 15833. (a) Effects of **1**–**4** on turbidity (OD_{620}) of culture medium. (b) Effects of **1**–**4** on the fluorescence Ex_{280}/Em_{490} values of bacterium-free supernatant. They were expressed as a percentage relative to that of the vehicle group. The error bars represent the SD ($n = 2$ or 3).

totoxicity should prompt further investigation of the structure–activity relationship in the cyclic peptide moiety to less toxic pyoverdine inhibitors.

According to the previous report (Maenaka *et al.* 2020), actinomycin D moderately reduced the turbidity of culture media, suggesting that it was toxic to *P. fluorescens* NBRC15833. However, it was difficult to determine whether this toxicity resulted from the suppression of pyoverdine production, inhibition of RNA synthesis, or another mechanism (Maenaka *et al.* 2020). In contrast, **1**–**4** appeared to promote bacterial growth, as indicated by increased turbidity in the presence of these compounds (Figure 4). It is also possible that these analogs induced morphological changes in the bacteria, as reported for other antibiotics (Eng, Smith and Cherubin 1984). Based on the limited reports on the biological activities of **4** (Meienhofer and Patel 1971; Moore *et al.* 1976), it may behave as a weak actinomycin-like antibiotic *in vitro*, while its *in vivo* antitumor profile may differ from that of actinomycin D. Thus, the cyclic peptide moiety may bind with unknown target molecules, or the pharmacodynamic profiles of **1**–**4** in mice and bacteria may differ from that of actinomycin D.

Conclusion

We synthesized actinomycin analogs (**1**–**3**) with modified phenoxazine moieties and the previously reported analog **4**. The actinomycin D cyclic depsipeptides in these analogs were replaced with cyclic peptides containing 2,3-diaminopropionic acid residues. Analogs **1** and **2**, without the phenoxazine ring, did not decrease the viability of HHUA cells, whereas **3** and **4** showed cytotoxicity, albeit 200–800 times weaker than that of actinomycin D. Only **4** retained pyoverdine production inhibitory activity against *P. fluorescens* NBRC15833, albeit an order of magnitude lower than actinomycin D. These results suggested that the phenoxazine ring was indispensable for cytotoxicity and pyoverdine production inhibitory activity. Further cyclic peptide modification is necessary to understand the structure–activity relationship of pyoverdine production inhibitory activity and develop preferable analogs that inhibit pyoverdine production with lower cytotoxicity.

Although actinomycins were first isolated as antibiotics with antitumor and cytotoxic activities, they have been found to participate in other biological activities, including discoidin domain receptors and pyoverdine production inhibitory activities (Siddiqui *et al.* 2009; Maenaka *et al.* 2020). The lactam analog **4** was synthesized and evaluated for anti-cancer effects in 1970s (Meienhofer and Patel 1971; Moore *et al.* 1976), but its pyoverdine production inhibitory activity was first demonstrated in this study. Our results suggest that structural modification can elicit a desirable activity from pleiotropic actinomycins. There may also be undiscovered biological activities of actinomycins; our less toxic actinomycin analogs (**1**–**4**) could be useful to explore unknown functions that are masked by the strong toxicity of actinomycins.

Experimental

General remarks

^{1}H and ^{13}C NMR spectra were recorded on JEOL JNM-ECZ500 and JNM-ECZ600R (JEOL, Tokyo, Japan) with chemical shifts reported in ppm relative to the residual solvent signals (^{1}H NMR:

Downloaded from academic.oup.com/bbb/article/90/10/1317/8735818 by guest on 26 September 2026

$CDCl_3$, δ = 7.26 ppm and methanol-d_4, δ = 3.30 ppm; ^{13}C NMR: $CDCl_3$, δ = 77.0 ppm and methanol-d_4, δ = 49.0 ppm). Optical rotations were measured with a P-1010 polarimeter (JASCO, Tokyo, Japan). High-resolution electrospray ionization mass spectra (HR-ESI-qTOF-MS) were obtained using a micrOTOF II (Bruker Daltonics, Billerica, MA, USA). Wakogel® C-300 (FUJIFILM Wako Pure Chemical Corporation, Osaka, Japan) was used for column chromatography. Silica gel 70 F_{254} TLC Plate-Wako (FUJIFILM Wako Pure Chemical Corporation) was used for preparative thin-layer chromatography (PTLC). All other reagents were purchased from FUJIFILM Wako Pure Chemical Corporation, Tokyo Chemical Industry (Tokyo, Japan), Watanabe Chemical Industries (Hiroshima, Japan), or Kanto Chemical (Tokyo, Japan).

Synthesis of 1–4

Synthesis of 8

$SOCl_2$ (0.800 mL, 11.1 mmol) was added to a solution of **6** (2.35 g, 9.88 mmol) in MeOH (50 mL) at 0 °C. The reaction mixture was stirred at 0 °C for 2 h. At that point, additional $SOCl_2$ (0.290 mL, 4.02 mmol) was added. After stirring for 20 h at room temperature, the reaction mixture was concentrated under reduced pressure to afford **7** (2.86 g). *N*,*N*-Diisopropylethylamine (DIPEA) was added to a solution of Boc-MeVal-OH (2.29 g, 9.90 mmol), EDC·HCl (2.23 g, 11.6 mmol), and HOBt·H_2O (1.81 g, 11.8 mmol) in CH_2Cl_2 (40 mL) at 0 °C. After 10 min of stirring at 0 °C, a solution of **7** (2.86 g) in dimethylformamide (10 mL) was added. After stirring for 10 min at 0 °C followed by 20 h at room temperature, the reaction was quenched with 0.1 M aqueous solution of HCl (100 mL). The organic layer was separated, and the aqueous layer was extracted with hexane (100 mL) and 50% ethyl acetate (EtOAc) in hexane (100 mL × 2). The combined organic layers were washed with a saturated aqueous solution of $NaHCO_3$ and brine, dried over Na_2SO_4, filtered, and concentrated under reduced pressure. The residue was purified by column chromatography (silica gel, 30% → 50% EtOAc/hexane) to yield **8** (3.74 g, 8.03 mmol, 81% in 2 steps) as a colorless oil.

$[\alpha]_D$, –70 (*c* 1.0, MeOH, 27.4 °C). ^1H NMR (500 MHz, $CDCl_3$) δ 0.84 (3H, d, J = 6.3 Hz, Hγ of Mev), 0.90 (3H, d, J = 6.3 Hz, Hγ of Mev), 1.46 (9H, s, CH_3 of Boc), 2.19–2.24 (1H, m, Hβ of Mev), 2.73 (3H, s, NCH_3 of Mev), 3.47 (1H, d, J = 13.2 Hz, Hβ of Dap), 3.73 (3H, s, CO_2CH_3 of Dap), 3.84 (1H, d, J = 6.3 Hz, Hβ of Dap), 3.95 (1H, d, J = 11.5 Hz, Hα of Mev), 4.41 (1H, m, Hα of Dap), 5.08 (1H, d, J = 12.6 Hz, CH_2Ph of Cbz), 5.12 (1H, d, J = 12.1 Hz, CH_2Ph of Cbz), 5.81 (1H, d, J = 6.3 Hz, NH_α of Dap), 6.59 (1H, s, NH_β of Dap), 7.29–7.36 (5H, m, Ph of Cbz) ppm; ^{13}C NMR (126 MHz, $CDCl_3$) δ 18.4 (Cγ of Mev), 19.6 (Cγ of Mev), 25.7 (Cβ of Mev), 28.4 (3C, CH_3 of Boc), 29.9 (NCH_3 of Mev), 40.6 (Cβ of Dap), 52.7 (CO_2CH_3 of Dap), 54.5 (Cα of Dap), 64.5 (Cα of Mev), 67.0 (Ph of Cbz), 80.5 (C(CH_3)$_3$ of Boc), 128.0 (2C, Ph of Cbz), 128.1 (Ph of Cbz), 128.4 (Ph of Cbz), 136.1 (Ph of Cbz), 155.8 (Ph of Cbz), 157.3 (C = O of Boc), 170.6 (C = O of Dap), 171.5 (C = O of Mev) ppm. HR-ESI-MS: *m*/*z* 488.2352, ([M + Na]$^+$, calcd.for $C_{23}H_{35}N_3O_7Na$, 488.2367).

Synthesis of 11

LiOH·H_2O (107 mg, 2.55 mmol) was added to a solution of **8** (558 mg, 1.20 mmol) in MeOH (4 mL), THF (4 mL), and H_2O (1 mL) at 0 °C. After 135 min of stirring at 0 °C, the reaction mixture was acidified with a 3M aqueous solution of HCl (2 mL). After MeOH was removed under reduced pressure, the residue was extracted with EtOAc (10 mL × 3), and the combined organic layers were washed with brine and dried over Na_2SO_4, filtered, and concentrated under reduced pressure to yield **9** (527 mg, 1.17 mmol, 97%). DIPEA (0.44 mL, 2.6 mmol) was added to a solution of **9** (527 mg, 1.17 mmol), EDC·HCl (244 g, 1.27 mmol), and HOBt·H_2O (1.85 g, 12.0 mmol) in CH_2Cl_2 (3 mL) at 0 °C. After 6 min of stirring at 0 °C, a solution of **10** (346 mg, 1.01 mmol) in CH_2Cl_2 (2 mL) was added. After further stirring for 10 min at 0 °C followed by 22 h at room temperature, the reaction was quenched with 0.1 M aqueous solution of HCl (10 mL). The mixture was extracted with CH_2Cl_2 (6 mL) and EtOAc (40 mL). The combined organic layer was washed with a saturated aqueous solution of $NaHCO_3$ and brine, dried over Na_2SO_4, filtered, and concentrated under reduced pressure. The residue was purified by column chromatography (silica gel, 0% → 5% EtOAc/hexane) to yield **11** (432 mg, 0.557 mmol, 55%) as a white solid.

$[\alpha]_D$, –70 (*c* 0.65, MeOH, 27.4 °C). ^1H NMR (500 MHz, $CDCl_3$, mixture of rotamers) δ 0.80–0.92 (12H, m), 1.39–1.50 (18H, m), 1.91–2.01 (3H, m), 2.07–2.22 (3H, m), 2.70–2.80 (3H, m), 2.92–2.96 (1H, m), 3.10–3.12 (2H, m), 3.22–3.29 (1H, m), 3.54–4.06 (5H, m), 4.22 (1H, s), 4.56–4.60 (1H, m), 4.76–4.84 (1H, m), 5.05–5.14 (2H, m), 7.26–7.34 (5H, m) ppm; ^{13}C NMR (126 MHz, $CDCl_3$, mixture of rotamers) δ 14.1, 17.6, 18.5, 18.6, 19.4, 19.4, 19.6, 19.6, 19.6, 19.7, 21.0, 24.3, 26.2, 28.0, 28.1, 28.4, 29.1, 29.9, 30.0, 30.6, 30.9, 31.0, 35.6, 36.1, 36.4, 41.0, 41.0, 47.5, 47.6, 50.4, 50.5, 50.7, 55.7, 56.2, 56.7, 57.3, 60.4, 63.9, 63.9, 67.0, 127.9, 128.0, 128.1, 128.2, 128.2, 128.4, 128.4, 128.5, 136.9, 156.7, 156.7, 167.9, 168.4, 169.8, 169.8, 169.9, 169.9, 170.0, 170.2, 171.2, 171.8, 172.3, 172.3, 172.8, 173.1 ppm. HR-ESI-MS: *m*/*z* 797.4416, ([M + Na]$^+$, calcd.for $C_{39}H_{62}N_6O_{10}Na$, 797.4420).

Synthesis of 13

A 4 M solution of HCl in dioxane (8 mL) was added to **11** (101 mg, 0.130 mmol) in a flask, and the reaction mixture was stirred at room temperature for 22 h. The mixture was concentrated under reduced pressure to yield a residue containing **12**. DIPEA (0.15 mL, 0.88 mmol) was added to a solution of this residue in CH_2Cl_2 (100 mL) at 0 °C. HATU (148 mg, 0.390 mmol) was added after 20 min of stirring at 0 °C. After further stirring for 20 min at 0 °C and 22 h at room temperature, the reaction was quenched with 1 M aqueous solution of HCl (100 mL). The organic layer was separated, washed with a saturated aqueous solution of $NaHCO_3$ and brine, dried over Na_2SO_4, filtered, and concentrated under reduced pressure. The residue was purified by column chromatography (silica gel, 0% → 10% MeOH/EtOAc) to yield **13** (62.1 mg, 0.103 mmol, 79% in 2 steps) as a white solid.

$[\alpha]_D$, –61 (*c* 0.44, MeOH, 27.4 °C). ^1H NMR (500 MHz, $CDCl_3$, mixture of rotamers) δ 0.79–0.92 (9H, m, Hγ of Val, Hγ of Mev), 1.02 (3H × 0.6, d, J = 6.3 Hz, Hγ of Val, Hγ of Mev), 1.15 (3H × 0.4, d, J = 6.3 Hz, Hγ of Val, Hγ of Mev), 1.85–2.11 (4H, m, Hβ and Hγ of Pro, Hβ of Val), 2.17–2.41 (2H, m, Hβ of Pro, Hβ of Mev), 2.69 (3H × 0.6, s, NCH_3 of Mev), 2.90 (3H × 0.4, s, NCH_3 of Mev), 3.13 (1H × 0.6, d, J = 14.9 Hz, Hα of Sar), 3.17 (1H × 0.4, d, J = 14.3 Hz, Hα of Sar), 3.26 (3H × 0.6, s, NCH_3 of Sar), 3.36 (3H × 0.4, s, NCH_3 of Sar), 3.50 (1H, t, J = 14.9 Hz, Hβ of Dap), 3.59–3.66 (1H, m, Hδ of Pro), 4.16–4.34 (4H, m, Hα of Mev, Hδ of Pro, Hα and Hβ of Dap), 4.38 (1H × 0.4, t, J = 10.3 Hz, Hα of Val), 4.49 (1H × 0.6, t, J = 10.3 Hz, Hα of Val), 4.58 (1H, d, J = 14.3 Hz, Hα of Sar), 4.76 (1H × 0.6, dd, J = 8.6, 4.0 Hz, Hα of Pro), 4.84 (1H × 0.4, dd, J = 8.6, 4.0 Hz, Hα of Pro), 5.04 (1H, d, J = 12.6 Hz, CH_2Ph of Cbz), 5.19 (1H, d, J = 12.0 Hz, CH_2Ph of Cbz), 7.29–7.35 (5H, m, Ph of Cbz), 8.34 (1H, d, J = 9.7 Hz, NH_α of Dap) ppm; ^{13}C NMR (126 MHz, $CDCl_3$, mixture of rotamers) δ 18.4 (Cγ of Val or Cγ of Mev), 18.6 (Cγ of Val or Cγ of Mev), 18.7 (Cγ of Val or Cγ of Mev), 19.2 (Cγ of Val or Cγ of Mev), 20.4 (Cγ of Val or Cγ of Mev), 21.4 (Cγ of Val or Cγ of Mev), 24.6 (Cγ of Pro, minor),

Downloaded from academic.oup.com/bbb/article/90/10/1317/8735818 by guest on 26 September 2026

24.7 (Cγ of Pro, major), 26.2 (Cβ of Mev, major), 27.3 (Cβ of Mev, minor), 27.7 (Cβ of Pro, major), 28.6 (Cβ of Pro, minor), 29.0 (NCH_3 of Mev, major), 29.3 (Cβ of Val, major), 29.4 (Cβ of Val, minor), 32.5 (NCH_3 of Mev, minor), 37.9 (NCH_3 of Sar, major), 39.0 (NCH_3 of Sar, minor), 39.9 (Cβ of Dap, major), 40.7 (Cβ of Dap, minor), 47.7 (Cδ of Pro, minor), 48.1 (Cδ of Pro, major), 50.1 (Cα of Sar, major), 50.2 (Cα of Sar, minor), 54.9 (Cα of Dap, major), 56.5 (Cα of Pro, minor), 56.7 (Cα of Val, minor), 56.8 (Cα of Val, major), 57.0 (Cα of Dap, minor), 57.6 (Cα of Pro, major), 61.7(Cα of Mev, minor), 66.6 (Cα of Mev, major), 67.0 and 67.4 (CH_2Ph of Cbz), 128.1, 128.2, 128.3, 128.4, 128.5, 136.0, 136.4 (Ph of Cbz), 156.0 and 156.4 (C = O of Cbz), 169.4 (C = O of Sar), 170.7 (C = O of Mev), 171.0 (C = O of Dap), 171.4 (C = O of Val), 173.3 (C = O of Pro) ppm. HR-ESI-MS: *m*/*z* 623.3177, ($[M + Na]^+$, calcd.for $C_{30}H_{44}N_6O_7Na$, 623.3164).

Synthesis of 5

10% Pd/C (6.5 mg) was added to a solution of **13** (66.5 mg, 1.13 mmol) in MeOH (1.4 mL) at room temperature. The reaction mixture was stirred for 2 h under an H_2 atmosphere at room temperature. The mixture was filtered, and the filtrate was concentrated under reduced pressure to yield **5** (53.1 mg, 1.13 mmol, quant) as a white solid.

$[\alpha]_D$, –99 (*c* 0.43, MeOH, 18.8 °C). ^{1}H NMR (500 MHz, $CDCl_3$, mixture of rotamers) δ 0.80 (3H × 0.7, d, *J* = 6.9 Hz, Hγ of Mev), 0.83 (3H × 0.3, d, *J* = 6.9 Hz, Hγ of Mev), 0.90–0.98 (6H, m, Hγ of Val), 1.02 (3H × 0.7, d, *J* = 6.3 Hz, Hγ of Mev), 1.13 (3H × 0.3, d, *J* = 6.3 Hz, Hγ of Mev), 1.86–2.00 (3H, m, Hβ and Hγ of Pro), 2.06–2.24 (1H, m, Hβ of Val), 2.26-2.30 (1H, m, Hβ of Pro), 2.36–2.42 (1H, m, Hβ of Mev), 2.70 (3H × 0.7, s, NCH_3 of Mev), 2.89 (3H × 0.3, s, NCH_3 of Mev), 3.10 (1H × 0.7, d, *J* = 14.3 Hz, Hα of Sar), 3.17 (1H × 0.3, d, *J* = 14.3 Hz, Hα of Sar), 3.26 (3H × 0.7, s, NCH_3 of Sar), 3.37 (3H × 0.3, s, NCH_3 of Sar), 3.53 (1H, d, *J* = 13.7 Hz, Hβ of Dap), 3.58 (1H, d, *J* = 5.1 Hz, Hα of Dap), 3.61–3.65 (1H, m, Hδ of Pro), 4.09–4.37 (3H, m, Hβ of Dap, Hα of Mev, Hδ of Pro), 4.48 (1H, t, *J* = 10.3 Hz, Hα of Val), 4.59 (1H × 0.3, d, *J* = 14.3 Hz, Hα of Sar), 4.62 (3H × 0.7, d, *J* = 13.7 Hz, Hα of Sar), 4.80 (1H × 0.7, dd, *J* = 9.7, 4.6 Hz, H-Pα), 4.87 (1H × 0.3, dd, *J* = 8.6, 4.0 Hz, H-Pα), 7.75 (1H, d, *J* = 9.8 Hz, N*H* of Val), 8.22 (1H, d, *J* = 10.3 Hz, N*H* of Dap) ppm; ^{13}C NMR (126 MHz, $CDCl_3$, mixture of rotamers) peaks for major isomer: δ 18.7 (Cγ of Mev), 18.7 (Cγ of Val), 19.4 (Cγ of Val), 20.5 (Cγ of Mev), 24.7 (Cγ of Pro), 26.1 (Cβ of Mev), 27.7 (Cβ of Pro), 28.8 (NCH_3 of Mev), 29.1 (Cβ of Val), 37.8 (NCH_3 of Sar), 41.8 (Cβ of Dap), 48.0 (Cδ of Mev), 50.0 (Cα of Sar), 53.2 (Cα of Dap), 56.6 (Cα of Dap), 57.5 (Cα of Pro), 66.7 (Cα of Mev), 169.6 (C = O of Sar), 170.3 (C = O of Mev), 170.7 (C = O of Pro), 171.4 (C = O of Val), 172.9 (C = O of Dap) ppm. HR-ESI-MS: *m*/*z* 489.2794, ($[M + Na]^+$, calcd.for $C_{22}H_{38}N_6O_5Na$, 489.2796).

Synthesis of 1

A solution of isophthalic acid (4.3 mg, 0.026 mmol) and HATU (21.6 mg, 0.0568 mmol) in CH_2Cl_2 (0.5 mL) was added to DIPEA (0.02 mL, 0.1 mmol) at room temperature. After 10 min of stirring at the same temperature, a solution of **5** (24.0 mg, 0.0514 mmol) in CH_2Cl_2 (0.5 mL) was added. This reaction mixture was stirred at room temperature for 22 h before CH_2Cl_2 (7 mL) and 1 M aqueous solution of HCl (7 mL) were added. The formed organic layer was separated, washed with a saturated aqueous solution of $NaHCO_3$ and brine, dried over Na_2SO_4, filtered, and concentrated under reduced pressure. The residue was purified by column chromatography (silica gel, 0% → 50%) to yield **1** (11.5 mg, 0.0108 mmol, 42%) as a white solid.

$[\alpha]_D$, –44 (*c* 0.092, MeOH, 27.4 °C). ^{1}H NMR (500 MHz, methanol-d_4, mixture of rotamers) δ 0.84-1.28 (24H, m), 1.82–2.08 (8H, m), 2.22–2.43 (4H, m), 2.67–2.94 (6H, m) 3.04–3.45 (10H, m), 3.52–3.88 (4H, m), 4.01–4.29 (4H, m), 4.35–4.85 (10H, m), 7.52–7.62 (1H, m), 7.91–8.17 (2H, m), 8.30–8.49 (1H, m) ppm; ^{13}C NMR (150 MHz, methanol-d_4, mixture of rotamers) δ 17.1, 17.3, 17.4, 17.6, 19.1, 19.2, 19.2, 19.3, 19.6, 21.1, 22.4, 22.4, 25.7, 25.8, 27.5, 28.4, 28.4, 28.9, 29.5, 29.5, 30.1, 30.4, 30.5, 38.2, 38.9, 41.0, 41.7, 41.7, 50.8, 50.8, 57.3, 57.5, 57.7, 57.8, 58.3, 58.4, 58.4, 59.1, 59.3, 63.5, 67.8, 68.0, 126.9, 128.8, 131.5, 131.7, 135.7, 138.2, 147.9, 148.5, 168.5, 172.2, 172.3, 172.4, 172.6, 172.7, 173.5, 174.5, 177.2, 177.2 ppm. HR-ESI-MS: *m*/*z* 554.2833, 1085.5718 ($[M + Na_2]^{2+}$, calcd.for $C_{52}H_{78}N_{12}O_{12}Na_2$, 554.2823, $[M + Na]^+$, calcd.for $C_{52}H_{78}N_{12}O_{12}Na$, 1085.5754).

Synthesis of 2

A solution of 1,3-phenylenediacetic acid (4.4 mg, 0.023 mmol) and HATU (18.5 mg, 0.0487 mmol) in CH_2Cl_2 (0.5 mL) was added to DIPEA (0.02 mL, 0.1 mmol) at room temperature. After 10 min of stirring at the same temperature, a solution of **5** (20.9 mg, 0.0448 mmol) in CH_2Cl_2 (0.5 mL) was added. This reaction mixture was stirred at room temperature for 21 h before CH_2Cl_2 (7 mL) and 1 M aqueous solution of HCl (7 mL) were added. The formed organic layer was separated, washed with a saturated aqueous solution of $NaHCO_3$ and brine, dried over Na_2SO_4, filtered, and concentrated under reduced pressure. The residue was purified by column chromatography (silica gel, 0% → 50%) to yield **2** (5.3 mg, 0.0049 mmol, 22%) as a white solid.

$[\alpha]_D$, –37 (*c* 0.15, MeOH, 27.4 °C). ^{1}H NMR (500 MHz, methanol-d_4, mixture of rotamers) δ 0.81–1.15 (24H, m), 1.82–2.12 (8H, m), 2.22–2.42 (4H, m), 2.66–2.92 (6H, m), 3.05–3.28 (4H, m), 3.33–3.40 (4H, m), 3.45–3.80 (10H, m), 4.06–4.24 (4H, m), 4.32–4.86 (8H, m), 7.10–7.32 (4H, m) ppm; ^{13}C NMR (150 MHz, methanol-d_4, mixture of rotamers) δ 14.4, 17.2, 17.3, 17.4, 18.4, 19.0, 19.1, 19.2, 19.3, 19.4, 19.7, 21.1, 23.7, 25.6, 25.7, 27.4, 28.9, 29.4, 29.6, 30.0, 30.5, 32.8, 38.2, 38.8, 30.7, 41.1, 41.3, 43.7, 49.6, 50.7, 53.6, 56.3, 57.3, 57.5, 57.8, 58.3, 58.4, 59.0, 59.3, 67.8, 120.9, 127.6, 128.3, 128.6, 128.7, 128.7, 128.9, 128.9, 129.9, 130.1, 131.2, 136.6, 136.7, 136.8, 148.6, 150.3, 171.7, 172.0, 172.0, 172.1, 172.2, 172.4, 172.6, 174.2 ppm. HR-ESI-MS: *m*/*z* 568.2956, 1113.6047 ($[M + Na_2]^{2+}$, calcd.for $C_{54}H_{82}N_{12}O_{12}Na_2$, 568.2980, $[M + Na]^+$, calcd.for $C_{54}H_{82}N_{12}O_{12}Na$, 1113.6067).

Synthesis of 14

A solution of 2-nitro-3-(phenylmethoxy)benzoic acid (40.5 mg, 0.148 mmol) and HATU (64.0 mg, 0.168 mmol) in CH_2Cl_2 (2 mL) was added to DIPEA (0.06 mL, 0.3 mmol) at 0 °C. After 10 min of stirring at 0 °C, a solution of **5** (52.6 mg, 0.113 mmol) in CH_2Cl_2 (2 mL) was added. This reaction mixture was stirred at room temperature for 21 h before 1 M aqueous solution of HCl (5 mL) was added. The mixture was extracted with EtOAc (15 mL), washed with a saturated aqueous solution of $NaHCO_3$ and brine, dried over Na_2SO_4, filtered, and concentrated under reduced pressure. The residue was purified by column chromatography (silica gel, 0% → 10% MeOH/EtOAc) to yield **14** (66.9 mg, 0.0927 mmol, 82%) as a white solid.

$[\alpha]_D$, +13 (*c* 0.52, MeOH, 26.1 °C). ^{1}H NMR (500 MHz, methanol-d_4, mixture of rotamers) δ 0.82 (3H × 0.6, d, *J* = 6.9 Hz, Hγ of Mev), 0.84 (3H × 0.4, d, *J* = 6.3 Hz, Hγ of Mev), 0.93 (3H × 0.6, d, *J* = 6.9 Hz, Hγ of Val), 0.96 (3H × 0.4, d, *J* = 6.9 Hz, Hγ of Val), 1.00 (3H × 0.4, d, *J* = 6.3 Hz, Hγ of Val), 1.04 (3H × 0.6, d, *J* = 7.4 Hz, Hγ of Val), 1.05 (3H × 0.6, d, *J* = 6.3 Hz, Hγ of Mev), 1.20 (3H × 0.4, d, *J* = 6.3 Hz, Hγ of Mev), 1.84–1.90 (1H, m, Hβ of Pro), 1.93–2.14 (3H, m, Hγ of Pro, Hβ of Val), 2.25–2.40 (2H, m, Hβ of Pro, Hβ of Mev), 2.65 (3H × 0.6, s, NCH_3 of Mev), 2.90 (3H × 0.4, s, NCH_3 of Mev), 3.25 (3H × 0.6, s, NCH_3 of Sar), 3.26–3.27 (1H, m, Hα of Sar), 3.31 (3H × 0.4, s, NCH_3

Downloaded from academic.oup.com/bbb/article/90/10/1317/8735818 by guest on 26 September 2026

of Sar), 3.46 (1H × 0.6, d, J = 13.7 Hz, Hβ of Dap), 3.60 (1H × 0.4, d, J = 13.7 Hz, Hβ of Dap), 3.67–3.76 (1H, m, Hδ of Pro), 4.08–4.29 (2H, m, Hβ of Dap, Hδ of Pro), 4.39–4.86 (5H, m, Hα of Val, Hα of Mev, Hα of Dap, Hα of Sar, Hα of Pro), 5.06–5.30 (2H, m, CH_2Ph of Bn), 7.10–7.53 (8H, m, aromatic) ppm; ^{13}C NMR (126 MHz, methanol-d_4, mixture of rotamers) δ 19.0, 19.1, 19.2, 19.3, 19.3, 19.5, 21.2, 22.4, 25.6, 25.7, 25.7, 25.8, 27.4, 28.8, 28.9, 29.4, 29.6, 30.2, 30.3, 30.7, 38.2, 38.8, 40.4, 40.5, 41.3, 49.6, 49.8, 50.6, 53.8, 55.8, 58.5, 58.6, 59.1, 59.3, 67.8, 67.9, 67.9, 72.2, 72.3, 118.8, 118.9, 120.7, 120.9, 122.1, 128.4, 128.5, 128.5, 129.0, 129.3, 129.3, 129.4, 129.4, 129.5, 129.7, 129.9, 132.7, 132.8, 133.4, 137.0, 137.1 140.8, 151.5, 151.6, 151.7, 152.1, 166.5, 167.2, 171.0, 171.8, 172.1, 172.3, 172.4, 172.5, 172.7, 173.4, 174.1, 174.4 ppm. HR-ESI-MS: m/z 744.3326, ([M + Na]$^+$, calcd.for $C_{36}H_{47}N_7O_9$Na, 744.3327).

Synthesis of 3

10% Pd/C (7.5 mg) was added to a solution of **14** (54.1 mg, 0.0750 mmol) in MeOH (1.3 mL) at room temperature. The reaction mixture was stirred for 5 h under an H_2 atmosphere at room temperature. The mixture was filtered, and the filtrate was concentrated under reduced pressure to yield **16** (49.7 mg). A solution of K_3[Fe(CN)$_6$] (62 mg, 0.19 mmol) in phosphate buffer saline (1.3 mL) was added to a solution of **16** (40.7 mg) in MeOH (1.1 mL). A 0.13 M aqueous solution of NaOH was added to adjust the pH to 7. After 20 h of stirring at room temperature, MeOH was removed under reduced pressure. The residue was extracted with EtOAc (5 mL × 3). The combined organic layer was washed with brine, dried over Na_2SO_4, filtered, and concentrated under reduced pressure. The residue was purified by column chromatography (silica gel, 0% → 50% MeOH/EtOAc) to yield **3** (6.2 mg, 0.0052 mmol, 14%) containing trace impurities. For biological evaluation, half of the product (3.1 mg) was further purified by PTLC (silica gel, 30% MeOH/EtOAc), yielding **3** (2.8 mg) as an orange solid.

[α]$_D$, –48 (c 0.21, MeOH, 30.1 °C). ^{1}H NMR (500 MHz, methanol-d_4, mixture of rotamers) δ 0.79–1.00 (18H, m), 1.15–1.22 (6H, m), 1.89–2.35 (12H, m), 2.50–2.92 (12H, m), 3.25–3.45 (4H, m), 3.67–3.73 (2H, m), 3.88–4.12 (6H, m), 4.28–4.36 (2H, m), 4.55–4.66 (4H, m), 5.95–6.10 (2H, m), 6.44 (1H, s), 7.54–7.60 (2H, m), 7.90 (1H, m) ppm; ^{13}C NMR (126 MHz, methanol-d_4, mixture of rotamers) δ 14.4, 19.4, 19.5, 19.7, 19.8, 20.3, 20.5, 23.7, 24.0, 24.1, 26.9, 26.9, 28.1, 28.3, 28.4, 30.2, 30.3, 30.3, 30.4, 30.5, 30.6, 30.6, 30.7, 30.7, 30.8, 30.8, 30.8, 32.0, 32.5, 35.6, 35.6, 36.5, 39.8, 39.9, 42.8, 43.0, 49.6, 53.1, 55.3, 55.4, 57.6, 58.9, 59.1, 59.5, 59.6, 78.6, 78.9, 79.1, 105.3, 106.5, 106.6, 107.5, 108.0, 119.7, 120.3, 128.5, 129.9, 130.8, 130.9, 131.2, 133.4, 143.2, 151.3, 168.1, 170.2, 170.5, 170.6, 171.2, 173.8, 174.4, 174.9, 175.3, 175.3, 180.4 ppm. HR-ESI-MS: m/z 1219.5871, ([M + Na]$^+$, calcd.for $C_{58}H_{80}N_{14}O_{14}$Na, 1219.5870).

Synthesis of 15

A solution of 4-methyl-2-nitro-3-(phenylmethoxy)benzoic acid (31.5 mg, 0.110 mmol) and HATU (61.5 mg, 0.162 mmol) in CH_2Cl_2 (2 mL) was added to DIPEA (0.12 mL, 0.69 mmol) at 0 °C. After 10 min of stirring at 0 °C, a solution of **5** (38.1 mg, 0.0817 mmol) in CH_2Cl_2 (3 mL) was added. This reaction mixture was stirred at room temperature for 22 h, before 1 M aqueous solution of HCl (6 mL) was added. The mixture was extracted with EtOAc (23 mL), washed with a saturated aqueous solution of $NaHCO_3$ and brine, dried over Na_2SO_4, filtered, and concentrated under reduced pressure. The residue was purified by column chromatography (silica gel, 33% EtOAc/hexane → 50% MeOH/EtOAc) to yield **15** (55.4 mg, 0.0753 mmol, 92%) as a white solid.

[α]$_D$, –3.3 (c 0.79, MeOH, 27.2 °C). ^{1}H NMR (500 MHz, methanol-d_4, mixture of rotamers) δ 0.84 (3H × 0.6, d, J = 7.4 Hz, Hγ of Mev), 0.86 (3H × 0.4, d, J = 6.3 Hz, Hγ of Mev), 0.93 (3H × 0.6, d, J = 6.9 Hz, Hγ of Val), 0.96 (3H × 0.4, d, J = 6.3 Hz, Hγ of Val), 0.99 (3H × 0.4, d, J = 6.9 Hz, Hγ of Val), 1.03 (3H × 0.6, d, J = 6.3 Hz, Hγ of Val), 1.10 (3H × 0.6, d, J = 6.3 Hz, Hγ of Mev), 1.23 (3H × 0.4, d, J = 6.3 Hz, Hγ of Mev), 1.86–1.90 (1H, m, Hβ of Pro), 1.94–2.13 (3H, m, Hγ of Pro, Hβ of Val), 2.29–2.41 (5H, m, Hβ of Pro, Hβ of Mev, PhCH_3), 2.67 (3H × 0.6, s, NCH_3 of Mev), 2.92 (3H × 0.4, s, NCH_3 of Mev), 3.25 (3H × 0.6, s, NCH_3 of Sar), 3.27 (1H, s, Hα of Sar), 3.32 (3H × 0.4, s, NCH_3 of Sar), 3.53 (1H, m, Hβ of Dap), 3.72 (1H, m, Hδ of Pro), 4.19–4.28 (2H, m, Hβ of Dap, Hδ of Pro), 4.38–4.48 (1H, m, Hα of Val), 4.50 (1H, d, J = 10.3 Hz, Hα of Mev), 4.54–4.77 (2H, m, Hα of Dap, Hα of Sar), 4.78–4.84 (1H, m, Hα of Pro), 4.94–5.08 (2H, m, CH_2Ph), 7.27–7.57 (7H, m, aromatic) ppm; ^{13}C NMR (126 MHz, methanol-d_4, mixture of rotamers) δ 16.4, 16.6, 16.7, 19.1, 19.2, 19.3, 19.3, 19.5, 21.3, 25.6, 25.8, 27.4, 27.4, 28.9, 29.4, 29.6, 30.3, 30.6, 38.3, 38.8, 40.5, 41.4, 49.6, 50.8, 54.0, 58.4, 58.6, 59.0, 59.2, 67.9, 77.8, 77.9, 78.0, 124.4, 124.6, 126.8, 129.0, 129.3, 129.4, 129.4, 129.5, 129.5, 129.6, 129.6, 130.0, 133.1, 134.3, 134.9, 137.4, 137.4, 139.2, 139.4, 145.7, 146.1, 150.2, 150.4, 166.2, 166.9, 171.1, 171.8, 172.2, 172.3, 172.4, 172.5, 172.7, 173.4, 174.2, 174.5 ppm. HR-ESI-MS: m/z 758.3463, ([M + Na]$^+$, calcd.for $C_{37}H_{49}N_7O_9$Na, 758.3484).

Synthesis of 4

10% Pd/C (5.3 mg) was added to a solution of **15** (32.5 mg, 0.0442 mmol) in MeOH (1 mL) at room temperature. This reaction mixture was stirred for 4 h under an H_2 atmosphere at room temperature. MeOH (4 mL) and 10% Pd/C (6.4 mg) were added, and the mixture was stirred for an additional 1.5 h under the same conditions. The mixture was filtered, and the filtrate containing **17** was added to MeOH (2 mL) and a solution of K_3[Fe(CN)$_6$] (52.2 mg, 0.158 mmol) in phosphate buffer saline (10 mL). After 20 h of stirring at room temperature, H_2O (25 mL) was added. The mixture was extracted with EtOAc (18 mL × 3). The combined organic layer was washed with brine, dried over Na_2SO_4, filtered, and concentrated under reduced pressure. The residue was purified by column chromatography (silica gel, 0% → 40% MeOH/EtOAc) followed by PTLC (silica gel, 7% MeOH/CH_2Cl_2) to yield **4** (4.2 mg, 0.0034 mmol, 15%) as an orange solid.

[α]$_D$, –161 (c 0.25, MeOH, 27.1 °C). ^{1}H NMR (500 MHz, methanol-d_4, mixture of rotamers) δ 0.79–0.99 (18H, m), 1.18–1.21 (6H, m), 1.86–2.35 (15H, m), 2.54–2.90 (15H, m), 3.27–3.48 (4H, m), 3.62–3.73 (2H, m), 3.87–4.14 (6H, m), 4.25–4.68 (6H, m), 5.95–6.04 (2H, m), 7.44 (1H, m), 7.79 (1H, m) ppm; ^{13}C NMR (126 MHz, methanol-d_4, mixture of rotamers) δ 15.1, 19.5, 19.6, 19.7, 19.7, 19.8, 20.4, 20.5, 24.0, 24.1, 28.3, 28.4, 30.8, 32.1, 32.3, 32.4, 32.5, 35.6, 39.8, 39.9, 42.7, 43.1, 49.6, 53.1, 55.4, 58.9, 59.1, 59.5, 59.6, 78.5, 79.1, 99.7, 114.4, 127.7, 130.0, 130.7, 130.9, 131.1, 151.5, 167.1, 168.3, 170.2, 170.6, 170.8, 171.3, 173.2, 173.8, 174.5, 174.9, 175.3, 175.3, 180.2 ppm. HR-ESI-MS: m/z 1247.6184, ([M + Na]$^+$, calcd.for $C_{60}H_{84}N_{14}O_{14}$Na, 1247.6184).

Cell culture

The HHUA (RCB0658) human endometrial cancer cell line was provided by the RIKEN BRC Bio-Resource Project of the NEXT/AMED (Tsukuba, Japan). HHUA cells were cultured in Ham's F-12 medium with 10% heat-inactivated fetal bovine serum, 1-mM L-glutamine, 100-U/mL penicillin, and 100-μg/mL streptomycin. They were maintained at 37 °C in a humidified atmosphere containing 5% CO_2.

Downloaded from academic.oup.com/bbb/article/90/10/1317/8735818 by guest on 26 September 2026

Cytotoxicity assay

HHUA cells (1.0×10^4 cells per 200 µL well) were seeded in a 96-well plate and allowed to attach overnight. Thereafter, a solution of each compound in DMSO or DMSO alone was added to each well. After a 24 h incubation, 20 μL of Cell Counting Kit-8 (FUJIFILM Wako Pure Chemical Corporation) was added to each well, and the plate was incubated at 37 °C for an additional 4 h. The absorbance at 450 nm was measured for the control (*C*) and test (*T*) wells using a microplate reader (Multiskan FC; Thermo Fisher Scientific, Waltham, MA, USA). Cell viability in the presence of each compound was calculated as $100 \times (T/C)$ using the average of four points. The IC_{50} value, defined as $100 \times (T/C) = 50$, was determined by processing these values.

Bacterial culture

Pseudomonas fluorescens NBRC 15833 was obtained from the Biological Resource Center, National Institute of Technology and Evaluation (NBRC). The bacteria were cultured in a medium containing hipolypepton (1 g), yeast extract (0.2 g), and $MgSO_4 \cdot 7H_2O$ (0.1 g) in H_2O (100 mL) at 30 °C.

Inhibition assay for pyoverdine production

Pyoverdine production inhibitory activity was evaluated as reported previously (Maenaka *et al.* 2020). *Pseudomonas fluorescens* NBRC 15833 was suspended in iron-limited Gassner's medium [L-asparagine·H_2O (0.2 g), D-glucose (0.7 g), $Na_2HPO_4 \cdot 12H_2O$ (243 mg), KH_2PO_4 (44 mg), and $MgSO_4 \cdot 7H_2O$ (20 mg) in 100 mL of H_2O] and diluted to an OD600 of 0.05. The bacterial suspension (2 mL) was transferred to a 15-mL centrifuge tube, and a solution of each compound (**1–4**) in DMSO or DMSO alone was added. The cultures were incubated at 30 °C for 24 h with shaking. After incubation, each suspension (200 μL) was transferred to a 96-well plate, and the absorbance at 620 nm was measured using a microplate reader (Multiskan FC; Thermo Fisher Scientific, Waltham, MA, USA). The bacterial cells were then precipitated, and the supernatant (100 μL) was transferred to a 96-well black plate. Fluorescence intensity (excitation wavelength 280 nm and emission wavelength 490 nm) was measured using a SpectraMax Gemini EM (Molecular Devices, San Jose, CA, USA).

Supplementary material

Supplementary material is available at *Bioscience, Biotechnology, and Biochemistry* online.

Data availability

The data supporting this study are available in the published article and its online supplementary material.

Author contribution

K.Y.: writing original draft, methodology, investigation, and analysis. Y. Hara: editing, methodology, and analysis. R.C.Y.: editing, methodology, and analysis. Y. Hanaki: conceptualization, writing original draft, methodology, and analysis.

Funding

This work was supported by the Kagawa University Research Promotion Program 2023 (Grant Number 23K0F013).

Disclosure statement

No potential conflict of interest was reported by the authors.

Acknowledgments

The authors thank Ms. Tsugumi Shiokawa and Dr. Hiroko Tada (Okayama University) for MS measurement and Assoc. Prof. Yukinari Sunatsuki (Okayama University) for NMR measurement.

References

Bai L, Chen P, Xiang J *et al.* Enantiomeric NMR discrimination of carboxylic acids using actinomycin D as a chiral solvating agent. *Org Biomol Chem* 2019;**17**:1466-70. https://doi.org/10.1039/C8OB03012J

Brockmann H, Seela F. Actinomycine. XXXVI; Synthesen von Actinomycinen und actinomycinähnlichen Chromopeptiden, IX 4.6-Didesmethyl-actinomycin C_1 und dessen 4.6-Dimethoxy-, 4.6-Diäthyl- und 4.6-Di-tert.-butyl-Derivat. *Chem Ber* 1971;**104**:2751-71. https://doi.org/10.1002/cber.19711040913

Chen J, Sun Z, Jin J *et al.* Role of siderophore in *Pseudomonas fluorescens* biofilm formation and spoilage potential function. *Food Microbiol* 2023;**109**:104151. https://doi.org/10.1016/j.fm.2022.104151

Chu W, Shinomiya M, Kamitori KY *et al.* Role of D-Valine residues in the antitumor drug actinomycin D: replacement of D-valines with other D-amino acids changes the DNA binding characteristics and transcription inhibitory activities. *J Am Chem Soc* 1994;**116**:7971-82. https://doi.org/10.1021/ja00097a003

Crowley DE, Wang YC, Reid CPP *et al.* Mechanisms of iron acquisition from siderophores by microorganisms and plants. *Plant Soil* 1991;**130**:179-98. https://doi.org/10.1007/BF00011873

Eng RH, Smith SM, Cherubin C. Inoculum effect of new beta-lactam antibiotics on *Pseudomonas aeruginosa*. *Antimicrob Agents Chemother* 1984;**26**:42-7. https://doi.org/10.1128/AAC.26.1.42

Kamitori S, Takusagawa F. Multiple binding modes of anticancer drug actinomycin D: x-ray, molecular modeling, and spectroscopic studies of d(GAAGCTTC)2-actinomycin D complexes and its host DNA. *J Am Chem Soc* 1994;**116**:4154-65. https://doi.org/10.1021/ja00089a002

Kirienko DR, Kang D, Kirienko NV. Novel pyoverdine inhibitors mitigate *Pseudomonas aeruginosa*. *Front Microbiol* 2018;**9**:3317. https://doi.org/10.3389/fmicb.2018.03317

Kirk JM. The mode of action of actinomycin D. *Biochimica et Biophysica Acta* 1960;**42**:167-9. https://doi.org/10.1016/0006-3002(60)90769-1

Lamont IL, Beare PA, Ochsner U *et al.* Siderophore-mediated signaling regulates virulence factor production in Pseudomonasaeruginosa. *Proc Natl Acad Sci USA* 2002;**99**:7072-7. https://doi.org/10.1073/pnas.092016999

Maenaka R, Tani S, Hikichi Y *et al.* Actinomycins inhibit the production of the siderophore pyoverdines in the plant pathogen Pseudomonas cichorii SPC9018. *Biosci Biotechnol Biochem* 2020;**84**:1975-85. https://doi.org/10.1080/09168451.2020.1785839

Mauger AB, Stuart OA. Slow *O,N*-acyl shift in an actinomycin-related peptide lactone. *Int J Peptide Protein Res* 1987;**30**:481-8. https://doi.org/10.1111/j.1399-3011.1987.tb03356.x

Mauger AB, Stuart OA, Ferretti JA *et al.* Conformation and dimerization of actinomycin-related peptide lactones in solution and in the solid state. *J Am Chem Soc* 1985;**107**:7154-63. https://doi.org/10.1021/ja00310a065

Downloaded from academic.oup.com/bbb/article/90/10/1317/8735818 by guest on 26 September 2026

Mauger AB, Stuart OA, Katz E. Synthesis and properties of some peptide analogues of actinomycin D. *J Med Chem* 1991;**34**:1297-301. https://doi.org/10.1021/jm00108a009

Meienhofer J. Syntheses of actinomycin and analogs. 3. A total synthesis of actinomycin D (Cl) via peptide cyclization between proline and sarcosine. *J Am Chem Soc* 1970;**92**:3771-7. https://doi.org/10.1021/ja00715a039

Meienhofer J, Patel RP. Synthesis of an actinomycin analog with substituted lactone oxygens (1',1'-bis(L-α,β-diaminopropionic acid))-actinomycin D (C 1). *Int J Protein Res* 1971;**3**:347-50. https://doi.org/10.1111/j.1399-3011.1971.tb01729.x

Minandri F, Imperi F, Frangipani E *et al.* Role of iron uptake systems in *Pseudomonas aeruginosa* virulence and airway infection. *Infect Immun* 2016;**84**:2324-35. https://doi.org/10.1128/IAI.00098-16

Moore S, Patel RP, Atherton E *et al.* Synthesis and some properties and antitumor effects of the actinomycin lactam analog, (di(1-L-α,β-diaminopropionic))actinomycin D^1. *J Med Chem* 1976;**19**:766-72. https://doi.org/10.1021/jm00228a006

Mosher CW, Lee DY, Enanoza RM *et al.* A phenazine analogue of actinomycin D. *J Med Chem* 1979;**22**:918-22. https://doi.org/10.1021/jm00194a006

Nakajima K, Tanaka T, Neya M *et al.* Studies on 2-aziridinecarboxylic acid. VIII. Total synthesis of actinomycin D and its serine analogue *via* ring-opening reaction of 1-benzyloxycarbonyl-2-aziridinecarboxylic acid moiety. *Bull Chem Soc Jpn* 1982;**55**:3237-41. https://doi.org/10.1246/bcsj.55.3237

Siddiqui K, Kim GW, Lee DH *et al.* Actinomycin D identified as an inhibitor of discoidin domain receptor 2 interaction with collagen through an insect cell based screening of a drug compound library. *Biol Pharmaceutical Bullet* 2009;**32**:136-41. https://doi.org/10.1248/bpb.32.136

Taguchi F, Suzuki T, Inagaki Y *et al.* The siderophore pyoverdine of *Pseudomonas syringae* pv. tabaci 6605 is an intrinsic virulence factor in host tobacco infection. *J Bacteriol* 2010;**192**:117-26. https://doi.org/10.1128/JB.00689-09

Takusagawa F, Dabrow M, Neidle S *et al.* The structure of a pseudo intercalated complex between actinomycin and the DNA binding sequence d(GpC). *Nature* 1982;**296**:466-9. https://doi.org/10.1038/296466a0

Visca P, Imperi F, Lamont IL. Pyoverdine siderophores: from biogenesis to biosignificance. *Trend Microbiol* 2007;**15**:22-30. https://doi.org/10.1016/j.tim.2006.11.004

Waksman SA, Woodruff HB. Bacteriostatic and bactericidal substances produced by a soil Actinomyces. *Exp Biol Med* 1940;**45**:609-14. https://doi.org/10.3181/00379727-45-11768

Wang X, Kleerekoper Q, Revtovich AV *et al.* Identification and validation of a novel anti-virulent that binds to pyoverdine and inhibits its function. *Virulence* 2020;**11**:1293-309. https://doi.org/10.1080/21505594.2020.1819144

Yao Z, Sun C, Xia Y *et al.* Mutasynthesis of antibacterial halogenated actinomycin analogues. *J Nat Prod* 2021;**84**:2217-25. https://doi.org/10.1021/acs.jnatprod.1c00294

Downloaded from academic.oup.com/bbb/article/90/10/1317/8735818 by guest on 26 September 2026

Received: 27 May 2026. **Accepted:** 13 July 2026

© The Author(s) 2026. Published by Oxford University Press on behalf of Japan Society for Bioscience, Biotechnology, and Agrochemistry. This is an Open Access article distributed under the terms of the Creative Commons Attribution License (https://creativecommons.org/licenses/by/4.0/), which permits unrestricted reuse, distribution, and reproduction in any medium, provided the original work is properly cited.